WAVEFRONT FIELDS IN THE SCATTERING OF ELASTIC WAVES BY SURFACE-BREAKING AND SUB-SURFACE CRACKS

Julius Miklowitz

California Institute of Technology
Pasadena, California 91125

INTRODUCTION

Of strong practical interest in the subject of fracture mechanics and related structural design and damage are the surface-breaking and sub-surface cracks. Indeed the scattered-wave fields generated by the interaction of incident surface or body waves with these cracks would be expected to yield most of the important information about the geometries of the cracks. It follows, in the subject of quantitative non-destructive evaluation (QNDE) there is considerable interest in scattering by surface-breaking and sub-surface cracks, as important steps in solving the inverse problems of obtaining the crack geometries from the scattered wave fields. However, having the solutions to the corresponding direct problems is a prerequisite to the inverse problems.

The present problems fall into a class that are nonseparable classically, and as such are difficult to solve. The nonseparability stems from media corners and crack edges. Mathematically, however, the boundary-value problems involved can be handled through integral transforms, integral equations, asymptotic and numerical analysis.

Recent Literature

The present problems were addressed recently in four important papers, three on the surface-breaking crack by Achenbach, Keer and Mendelsohn [1], Mendelsohn, Achenbach, and Keer [2] and Kundu and Mall [3]. The fourth paper by Achenbach and Brind [4] treated the sub-surface crack. In [1] and [2] the surface-breaking crack is assumed to be the two-dimensional normal edge-crack of

depth d in an elastic half plane, cf. Fig.1. In [4] the sub-surface crack is assumed to be the two-dimensional crack normal to the free surface of the elastic half plane with its tips at $y = a$ and $y = b$, respectively, where $b/a > 1$, cf. Fig.2. It was assumed also in these works that (1) the two faces of the cracks involved do not touch one another, hence these cracks never close completely, and (2) the loads and waves were time-harmonic in nature.

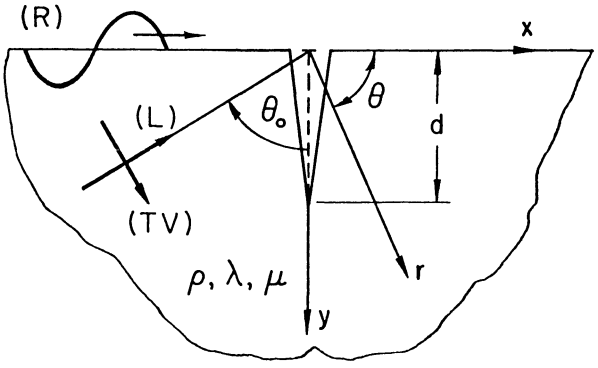

Fig.1. Waves incident on a surface-breaking crack of depth d (after Achenbach, Mendelsohn and Keer).

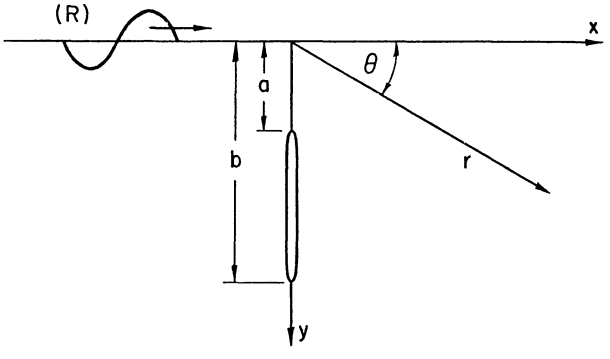

Fig. 2. Two dimensional sub-surface crack (after Achenbach and Brind).

The total field in the half plane for each of the problems in [1,2,4] is composed of the superposition of a specific incident field (say free surface or body waves) in the uncracked half-plane and the scattered field in the cracked half-plane generated by suitable surface tractions on the crack faces. Through equilibrium arguments in the plane of the crack these surface tractions are equal and opposite to the tractions generated by the incident wave in the uncracked half plane. Then by decomposing the scattered field into symmetric and antisymmetric fields with respect to the plane of the crack, one obtains a pair of boundary value problems for the quarter plane. Integral transform methods then reduce the two boundary value problems to two uncoupled singular integral equations which are solved numerically.

Numerical results presented graphically in [1] for the surface-breaking crack and an incident arbitrary (to a constant) Rayleigh surface wave disturbance, include variations of (i) normal and tangential crack-opening displacements with crack depth for three values of dimensionless frequency, (ii) crack-opening displacements at the mouth of the crack with dimensionless frequency, and (iii) Mode-I and Mode-II normalized dimensionless stress-intensity factors with dimensionless frequency. Considered here also were six different line loading configurations (through symmetries) applied at $(\mp x_1, 0)$ on the surface of the half plane about the crack and directed to the left or right of the crack, respectively. Then assuming that $k_R x_1 \gg 1$, only the surface motions due to these loads interact with the crack, k_R being the wave number of the Rayleigh surface waves. These loadings cause Mode-I or Mode II deformations. For example, normal crack-face loadings cause Mode-I deformations with symmetric displacements fields. Tangential crack-face loadings produce Mode-II deformations with antisymmetric displacements.

Numerical results were presented graphically in [2] for the surface-breaking crack and the following three types of incident arbitrary (to a constant) waves: (a) Rayleigh surface waves originating at $x=-\infty$, $y = 0$, (b) plane longitudinal waves originating at $r = \infty$, $0 \leq \theta_0 < \pi/2$, and (c) plane vertically polarized shear waves also originating at $r = \infty$, $0 \leq \theta_0 < \pi/2$, θ_0 being the angle of incidence, cf. Fig.1. For the incident Rayleigh surface wave disturbance, the numerical results included variations of the absolute values of the normalized horizontal and vertical displacements of the forward-and back-scattered surface waves with dimensionless frequency. For the incident plane longitudinal-and vertically polarized shear-waves the numerical results included variations of the forward-and back-scattered displacement fields with (i) the dimensionless frequency, for the angels of incidence $\theta_0 = 0°$, 30° and 60°, and (ii) the angle of incidence, for a low and high frequency.

Numerical results presented graphically in [4] for the sub-surface crack, and the case of an incident arbitrary (to constant)

Rayleigh surface wave disturbance, include variations of the dimensionless horizontal surface displacement in the (i) back-scattered, forward-scattered and transmitted Rayleigh waves with dimensionless frequency, for three values of a/b, (ii) back-scattered and transmitted Rayleigh waves with a/b, for three values of the dimensionless frequencies and (iii) phase shifts relative to the incident wave of the back-scattered and transmitted Rayleigh waves with dimensionless frequency, for the three values of a/b in (i) above. In addition numerical results were given for the normalized Mode-I and Mode-II stress intensity factors as a function of a/b for the three dimensional frequencies in (ii) above.

The paper by Kundu and Mal [3] is on the diffraction of elastic waves by a surface crack on a plate. The problem is that of a surface-breaking crack on one edge of the plate, one of plane strain and of time harmonic loads and waves, akin to the papers [1,2]. The incident waves are assumed to be either plane strain body waves (compressional P or shear SV) of arbitrary angle of propagation or surface Rayleigh waves propagating at right angles to the crack. The complete high frequency diffracted field on the plate surface is calculated for each incident wave. The solution is obtained by the application of an asymptotic theory of diffraction.

In [3] the following numerical results were displayed for the normalized x-component of the displacement on the plate surface $y=0$, due to various types of wave incidence, as a function of the dimensional frequency $k_1\ell = \omega\ell/c_1$ (ω, the frequency, c_1, the P wave speed). Curves included (i) amplitudes of transmitted, reflected and secondary shear converted Rayleigh waves for Poisson's ratio 1/3 and 1/4, (ii) Amplitudes of Rayleigh waves due to shear wave incidence at different angles for primary diffracted waves and secondary shear converted Rayleigh waves, (iii) shear wave incidence at different angles and (iv) body and surface waves of significant amplitude produced by incident P waves at 30°. A related interesting discussion of this data is presented.

Further, the reader should be aware of an important recent general work on the present subject, the ASME monograph on "Elastic waves and non-destructive testing of materials," edited by Y. H. Pao in 1978 [5].

Wavefront Analysis in the Nonseparable Elastodynamic Quarter-Plane Problems

Interestingly, Miklowitz has also published recently a two-part paper on wavefront analysis in the nonseparable elastodynamic quarter-plane problems [6]. This work involves loadings and waves (wavefronts) that are transient in nature, and therefore differs from the time-harmonic wave nature of the works [1,2,4] and [3]. However, the basic quarter-plane features of [1,2,4] and [6] are

similar, i.e., the boundary value problems of [1,2,4] are, in [6], boundary-initial value problems, the boundary (edge) conditions in [1,2,4] are like those in [6] except for the latter's time dependence. Integral transforms and related singular integral equations are a property of the solution techniques in both works, in which the solutions for these integral equations are found by numerical analysis [1,2,4] and by direct simple integrations yielding algebraic equations with following numeric evaluations [6]. It follows that the techniques in [6] can be applied to the quarter-plane problems in [1,2,4], hence giving the transient wavefront fields at their fronts and just behind them for regular wavefronts, as well as two-sided wavefronts involving a precursor, for these problems, i.e., the counterparts (high frequency pulses) of the solutions in [1,2,4]. The scattered transient wavefront fields obtained here then will be very valuable to the QNDE methods based on scattering of ultrasonic elastic waves by cracks, with interest towards solving the inverse problems of obtaining the crack geometries from these scattered transient wavefront fields.

Method of Solution. It has been pointed out earlier that the techniques in [6] can be applied to the quarter-plane problems in [1,2,4], hence giving the transient wavefront fields for these problems, i.e., the counterparts of the solutions in [1,2,4]. In order to reduce the text of [6, Parts 1 and 2] for the reader, the following sections contain main point consultations providing the necessary background for treating the present problems. The reader should be aware that this work is one of application of the basic techniques in [6] to the important surface-breaking and sub-surface crack problems.

General Quasi-Formal Solutions. First the governing equations for the general elastodynamic quarter-plane problem for plane strain are discussed, i.e., the coupled displacement partial differential equations of motion in $u(x,y,t)$ and $v(x,y,t)$ corresponding stress-strain relations, initial conditions and radiation conditions. This is followed by applying one-sided Laplace transforms in t, parameter p, and x, parameter s, to the displacement p.d. equations of motion in the now double-transformed displacements $\tilde{\bar{u}}(s,y,p)$ and $\tilde{\bar{v}}(s,y,p)$, cf. $(5)_1^*$, where the bar and tilda over quantities indicates L.T.'s on t and x, respectively. Solutions to these equations give the general quasi-formal solutions in terms of a double inversion integral involving both Bromwich paths, Br_p and Br_s, the p- and s-planes, respectively, cf. $(6a)_1$. Equations $(6b)_1$-$(6d)_1$ give $\tilde{\bar{u}}(s,y,p)$, $\tilde{\bar{v}}(s,y,p)$ with its complimentary functions $A_{\pm\alpha}$, $A_{\pm\beta}$ and particular integrals $\mu_{\pm\alpha}$, $\mu_{\pm\beta}$. The μ's are defined by integrals

*Here and hereafter subscript 1 on equation numbers indicates equations from [6, Partl], e.g., $(5)_1$.

which contain the time-transformed edge (x=0) unknowns (displacements and displacement gradients) through $f(s,y,p)$ and $g(s,y,p)$ the r.h. sides of $(5)_1$. These unknowns do become known quantities for particular problems later in the method, which then makes $(6a)_1$ a formal solution.

Associated with $(6a)_1$-$(6d)_1$ are the radiation conditions on y, according to $(4)_1$, which can be met with suitable values involving the α and β functions in $(6c)_1$. With interest in an s-plane inversion, we fix p and require that it be real and >0. Then as shown in [6, Part 1, Fig.2], taking cuts to the left from branch points $s=\pm k_s$, $\pm k_d$, we can represent analytic branches of $\alpha(s)$ and $\beta(s)$ through the equations $(7)_1$-$(10)_1$ for the Br_{sL} and Br_{sU} contours, respectively the lower and upper halves of Br_s. It follows then from $(9)_1$, that the multivalued functions $\alpha(s)$ and $\beta(s)$ satisfy $\mathrm{Re}\{{}^{\alpha(s)}_{\beta(s)}\} \geq 0$, for $\mathrm{Re}\{{}^{p}_{s}\} > 0$, on Br_{sL} (and Br_p), and hence, according to $(6b)_1$, will satisfy $(4)_1$ for $y \to \infty$, provided

$$A_{-\alpha(s)} = -\mu^{\infty}_{-\alpha(s)}(s,p)$$

and

$$A_{-\alpha(s)} = -\mu^{\infty}_{-\beta(s)}(s,p)$$

from $(11)_1$, which leads to the double-transformed displacements $\tilde{u}(s,y,p)$ and $\tilde{v}(s,y,p)$ in $(12)_1$ for Br_{sL}.

Similarly, from $(10)_1$, the multivalued functions $\alpha(s)$ and $\beta(s)$ satisfy $\mathrm{Re}\{{}^{\alpha(s)}_{\beta(s)}\} \leq 0$, for $\mathrm{Re}\{{}^{p}_{s}\} > 0$, on Br_{sU} (and Br_p), and hence, according to $(6b)_1$, will satisfy $(4)_1$ for $y \to \infty$, provided

$$A_{\alpha(s)} = \mu^{\infty}_{\alpha(s)} \quad ,$$

and

$$A_{\beta(s)} = \mu^{\infty}_{\beta(s)}$$

from $(13)_1$, which leads to the double-transformed displacements $\tilde{\tilde{u}}(s,y,p)$ and $\tilde{\tilde{v}}(s,y,p)$ in $(14)_1$ for Br_{sU}.

It is important to point out now that the branch functions $\alpha(s)$ and $\beta(s)$, defined in $(7)_1$ and $(8)_1$, respectively, are analytic all along Br_s, having $\mathrm{Re}[{}^{\alpha(s)}_{\beta(s)}] \geq 0$ on Br_{sL} from $(9)_1$ and

$\mathrm{Re}\begin{bmatrix}\alpha(s)\\ \beta(s)\end{bmatrix} \leq 0$ on Br_{sU} from $(10)_1$. Equations $(12)_1$ for $\tilde{\tilde{u}}$ and $\tilde{\tilde{v}}$ are bounded as $y \to \infty$ the critical terms being those involving $\exp[\alpha(s)y]$ and $\exp[\beta(s)y]$ where $\mathrm{Re}\begin{bmatrix}\alpha(s)\\ \beta(s)\end{bmatrix} \geq 0$ and the coefficients of these exponential functions vanish as $y \to \infty$. Similarly, $(14)_1$ for $\tilde{\tilde{u}}$ and $\tilde{\tilde{v}}$ are bounded as $y \to \infty$, the critical terms being those involving $\exp[-\alpha(s)y]$ and $\exp[-\beta(s)y]$ where $\mathrm{Re}\begin{bmatrix}\alpha(s)\\ \beta(s)\end{bmatrix} \leq 0$ and the coefficients of these exponential functions vanish as $y \to \infty$. It is of further interest to note from the results of $(9)_1$ and $(10)_1$, that according to the principle of reflection $\alpha(s)=-\alpha(s)$ and $\beta(s)=-\beta(s)$ on Br_{sU}, so that $(14)_1$ forms a natural conjugate of $(12)_1$. This leads to a real formal solution for the displacements over Br_{sL}, as well as other conjugations in the s-plane.

The Surface-Breaking Crack Problem. We now apply the basic techniques of [6], involving transient wavefront approximations to elastic waves scattered by cracks, to the problem of [1,2], i.e., the surface-breaking crack depicted in Fig.1. Then, as pointed out earlier the surface-breaking crack problem has a scattered field that decomposes into symmetric and antisymmetric fields with respect to the plane of the crack, generating a pair of boundary-value problems for the quarter plane. For the surface-breaking crack we have the following symmetric and antisymmetric boundary-initial value problems for the quarter plane,(cf. Fig.3).

$$\left.\begin{aligned} &\sigma_{xy}(0,y,t) = 0, && 0 \leq y < \infty \\ &\sigma_{x}(0,y,t) = -\sigma^{HT}_{xI}(0,y,t) && 0 \leq y < d \\ &u(0,y,t) = 0 \ , && d \leq y < \infty \end{aligned}\right\}, \ t > 0 \ , \qquad (1), (2), (3)$$

and

$$\left.\begin{aligned} &\sigma_{x}(0,y,t) = 0, && 0 \leq y < \infty \\ &\sigma_{xy}(0,y,t) = -\sigma^{HT}_{xyI}(0,y,t), && 0 \leq y < d \\ &v(0,y,t) = 0, && d \leq y < \infty \end{aligned}\right\}, \ t > 0 \qquad (4), (5), (6)$$

respectively, with the boundary conditions on $y = 0$,

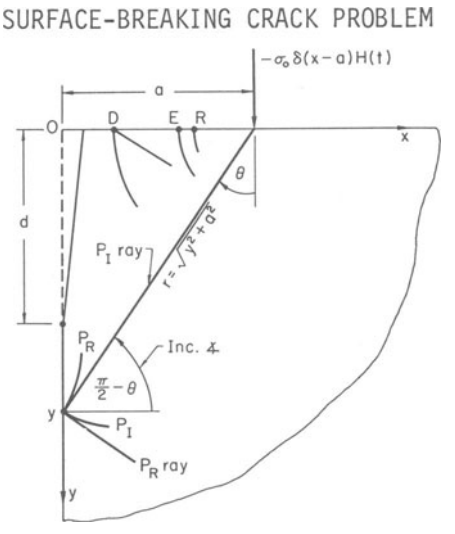

Fig.3. The quarter-plane free surface line loading and (1) the incident and reflected dilatational waves P_I and P_R it generates on the y-axis below the crack, and (2) the system of incident surface pulses, Dilatation D, Equivoluminal E and Rayleigh R it generates.

$$\left.\begin{aligned} \sigma_y(x,0,t) &= -\sigma_0\delta(x-a)H(t), \\ \sigma_{yx}(x,0,t) &= 0, \end{aligned}\right\} \quad x \geq 0,\ t > 0 \quad , \tag{7, 8}$$

applying to both of the above quarter-plane problems. In equations (1)-(8) u and v are the displacement components, and σ_x, σ_{xy} etc. are the stress components. In (2) and (5) the r.h. sides involve the total incident stress wave disturbances σ^{HT}_{xI} and σ^{HT}_{xyI}, subscript I indicating the incident compressional and vertically polarized shear wave nature of these stresses, respectively, the superscript H for H(t) the Heaviside step function, the time source in (7), and T for the total incident stress waves comprised of the incident and reflected (along the y-axis) components. Also in (7), σ_0 is the positive stress magnitude constant of the source of dimensions force per unit length, and $\delta(x-a)$ is the delta function representing the spatial singular normal line loading at $x = a$.

Concerning the sub-surface crack problem, the detail is very similar to the above surface-breaking crack case, and hence the latter problem will be treated separately in a later paper.

Analogous to the double transformed boundary conditions $(9)_1$ on $y = 0$, and the time-transformed boundary conditions $(10)_1$ on

we have from (7) and (8),

$$\tilde{\bar{\sigma}}_y(s,0,p)/(\lambda+2\mu) = (k^2-2)k^{-2}[s\tilde{\bar{u}}(s,0,p)-\bar{u}(0,0,p)]$$

$$+\tilde{\bar{v}}_y(s,0,p) = -\sigma_0 e^{-as}/(\lambda+2\mu)p \quad , \tag{9}$$

$$\tilde{\bar{\sigma}}_{yx}(s,0,p)/\mu = \tilde{\bar{u}}_y(s,0,p) + s\tilde{\bar{v}}(s,0,p) - \bar{v}(0,0,p) = 0 \tag{10}$$

where $k^2 = c_d^2/c_s^2$ with $c_d = (\lambda+2\mu/\rho)^{\frac{1}{2}}$ and $c_s = (\mu/\rho)^{\frac{1}{2}}$, the body wave speeds, and λ and μ are Lame's constants and ρ is the material density, and from (1), (2) and (3) of the symmetric boundary-initial value problem [the antisymmetric boundary-initial value problem will be similar involving (4)-(6)], we have

$$\bar{\sigma}_{xy}(0,y,p)/\mu = \bar{v}_x(0,y,p) + \bar{u}_y(0,y,p) = 0, \quad 0 \le y < \infty \quad , \tag{11}$$

$$\bar{\sigma}_x(0,y,p)/(\lambda+2\mu) = \bar{u}_x(0,y,p) + (k^2-2)k^{-2}\bar{v}_y(0,y,p)$$

$$= -\bar{\sigma}_{xI}^{HT}(0,y,p)/(\lambda+2\mu), \quad 0 \le y < d \quad , \tag{12}$$

and

$$\bar{u}(0,y,p) = 0 \quad , \quad d \le y < \infty \quad . \tag{13}$$

The stress $\bar{\sigma}_{xI}^{HT}(0,y,p)$ in (12) can be derived from the formal solution of Lamb's (half plane) problem with a line load surface source, represented here by the r.h.s. of (7). This solution in Cagniard-de Hoop form can be found in a variety of places including this writer's book [7], which is essentially de Hoop's treatment. From the formal solution, eq. (6.15) in [7], we can write

$$\begin{Bmatrix} \bar{u}_{xdI}^{H}(x,y,p) \\ \bar{v}_{ydI}^{H}(x,y,p) \end{Bmatrix} = \frac{\sigma_0 \bar{H}(p)}{2\pi\mu} \int_{-\infty}^{\infty} \begin{Bmatrix} \partial/\partial x \\ \partial/\partial y \end{Bmatrix} \left\{ \begin{bmatrix} f_d(\zeta) \\ h_d(\zeta) \end{bmatrix} e^{-pg_d(\zeta)} \right\} d\zeta \quad , \tag{14}$$

where

$$g_{\lambda}(\zeta) = (1/c_{\lambda})[\eta_{\lambda}'(\zeta)y - i\zeta(a-x)] \quad ,$$

$$f_d(\zeta) = i\zeta(k^2 + 2\zeta^2)/R(\zeta)\,, \quad h_d(\zeta) = \eta_d'(\zeta)(k^2 + 2\zeta^2)/R(\zeta)\,,$$

$$R(\zeta) = (k^2 + 2\zeta^2)^2 - 4\zeta^2\eta_d'(\zeta)\eta_s'(\zeta),$$

$$\eta_d'(\zeta) = \eta_d(\zeta)/k_d = (\zeta^2 + 1)^{1/2}, \eta_s'(\zeta) = \eta_s(\zeta)/k_d = (\zeta^2 + k^2)^{1/2},$$

and where "sub d and s" terms are associated with the dilatational and equivoluminal parts of the displacements, respectively, and $k_d = p/c_d$. In the interest of brevity here, at this point in the Cagniard-de Hoop inversion method, the reader is referred to [7, from the last paragraph on pg. 303 to the top of pg. 307 and eqs. (6.23),(6.24)]. It follows (14) is reduced to

$$\begin{Bmatrix} \bar{u}^H_{xdI}(x,y,p) \\ \bar{v}^H_{ydI}(x,y,p) \end{Bmatrix} = -\frac{\sigma_0}{\pi\mu c_d} \int_{r/c_d}^{\infty} \mathrm{Re}\left\{ \begin{Bmatrix} i\zeta_d f_d(\zeta_d) \\ \eta_d'(\zeta_d)h_d(\zeta_d) \end{Bmatrix} \frac{d\zeta_d}{dt} \right\} e^{-pt}\, dt, \quad (15)$$

where we have dropped the argument t of $\zeta_d(t)$. The integral equations in (15) are solved by inspection giving

$$\begin{Bmatrix} u^H_{xdI}(x,y,t) \\ v^H_{ydI}(x,y,t) \end{Bmatrix} = -\frac{\sigma_0}{\pi\mu c_d}\, \mathrm{Re}\left\{ \begin{Bmatrix} i\zeta_d f_d(\zeta_d) \\ \eta_d'(\zeta_d)h_d(\zeta_d) \end{Bmatrix} \Big/ g_d'(\zeta_d) \right\} H(t - r/c_d), \quad (16)$$

since it is easy to show $d\zeta_d/dt = 1/g_d'(\zeta_d)$, where the prime on g_d indicates the first derivative.

Making use now of a wavefront approximation technique due to Rosenfeld and Miklowitz [8], which is used in [7, § 6.2.1.4] we can obtain the dilatational wavefront approximations for the displacement gradients in (16). The approximations are obtained much as they are for the dilatational displacement wavefronts [7, pg. 319 to the top of pg. 321]. Basically exploiting the saddle point $\zeta_d = -i\zeta_0 = -i \sin\theta$, corresponding to the minimum time r/c_d, and expanding ζ_d away from $-i\zeta_0$, we obtain

$$\begin{Bmatrix} u^{H}_{xdI}(x,y,t) \\ v^{H}_{ydI}(x,y,t) \end{Bmatrix} = -\frac{\sigma_0}{\pi(2c_d)^{\frac{1}{2}}\mu} \left\{ \begin{Bmatrix} \sin^2\theta[f_d(-i\zeta_0)/\sin\theta] \\ \cos^2\theta[h_d(-i\zeta_0)/\cos\theta] \end{Bmatrix} \times [r(t-r/c_d)]^{-1/2} \right\} H(t-r/c_d) \tag{17}$$

where

$$f_d(-i\zeta_0) = \sin\theta(k^2 - 2\sin^2\theta)/R(-i\zeta_0) ,$$

$$h_d(-i\zeta_0) = \cos\theta(k^2 - 2\sin^2\theta)/R(-i\zeta_0) ,$$

$$R(-i\zeta_0) = (k^2 - 2\sin^2\theta)^2 + 4\sin^2\theta\cos\theta(k^2 - \sin^2\theta)^{1/2} ,$$

$$-\sin\theta = (a-x)/r , \quad \cos\theta = y/r , \quad r = (y^2 + a^2)^{1/2} ,$$

consistently with Fig. 3.

To complete $\bar{\sigma}^{HT}_{XI}(0,y,p)$ we need the reflected waves generated by the incident waves in (17) over the crack faces $0 \leq y < d$. The problem is the P-wave incidence case for plane harmonic or transient waves, which we assume holds on and near the y-axis as Fig. 3 shows. The reflection coefficients are

$$\frac{P_R}{P_I} = \frac{\sin 2\alpha \sin 2\beta - k^2\cos^2 2\beta}{\sin 2\alpha \sin 2\beta + k^2\cos^2 2\beta} ,$$

$$\frac{SV_R}{P_I} = -\frac{2\sin 2\alpha \cos 2\beta}{\sin 2\alpha \sin 2\beta + k^2\cos^2 2\beta} \tag{18}$$

where $\alpha = (\pi/2) - \theta$ is the angle of incidence w.r.t. the y-axis of P_I and angle of reflection of P_R, and β is the angle of reflection of SV_R. It follows that

$$\sin 2\alpha = 2\cos\theta\sin\theta , \quad \sin 2\beta = (2/k^2)\cos\theta(k^2 - \cos^2\theta)^{1/2} ,$$
$$\cos 2\beta = (k^2 - 2\cos^2\theta)/k^2 , \tag{19}$$

and substituting (19) into (18), we have from the latter the total incident system of wavefronts

$$P_I^T = P_I + P_R + SV_R = (1 + P_R/P_I + SV_R/P_I)P_I$$

$$= 4\left(\frac{2\cos\theta(k^2 - \cos^2\theta)^{1/2} - (k^2 - 2\cos^2\theta)}{4\cos\theta(k^2 - \cos^2\theta)^{1/2} + (k^2 - 2\cos^2\theta)^2/\sin\theta\cos\theta}\right)P_I \,, \qquad (20)$$

which can be identified with each of the incident displacement gradient wavefronts in (17). Then, using (20), and applying the Laplace transform on time for the strain, there results for the complete dimensionless transformed stress,

$$[\bar{\sigma}_{xI}^{HT}(0,y,p)/(\lambda+2\mu)]_{y \ll d}$$

$$= [\bar{u}_{xdI}^{HT}(0,y,p) + (k^2 - 2)k^{-2}\bar{v}_{ydI}^{HT}(0,y,p)]_{y \ll d}$$

$$\simeq \Sigma_0 y \cdot e^{-ap/c_d} p^{-1/2} \,, \qquad (21)$$

the r.h.s. of (21) is an expansion in y about $y = 0$, and the constant $\Sigma_0 = \sigma_0/(\pi a)^{3/2}(2c_d)^{1/2}(k^2 - 2)(\lambda + 2\mu)$. Equation (21) defines $\bar{\sigma}_{xI}^{HT}(0,y,p)/(\lambda + 2\mu)$ in (12).

To this point, we have dealt with the front running incident dilatational displacements and displacement gradient wavefronts, and the array of wavefronts they generate. Shortly after in time, similarly the incident equivoluminal displacement and displacement gradient wavefronts arrive, generating another system of wavefronts. Still later, the incident Rayleigh wave displacement and displacement gradient wavefronts arrive, generating still another system of wavefronts.

The later arriving incident equivoluminal and Rayleigh wavefronts can be handled like the foregoing dilatational wavefronts, cf. eqs. (14)-(21) and related text. The reader is further referred to [7, pp. 307 - top 309, eqs. (6.28), (6.32), and pp. bottom 310 - top 313, eqs. (6.39) - (6.42), (6.47)].

With these three different types of inputs for example, it will be of interest to learn, for the case of the free surface pulse incident to the quarter-plane corner, what the reflected wavefront is like for each of the incident surface pulses, e.g., surface pulses D, E, and R in Fig. 3. These surface pulses will be studied in later work.

Now, as in [6, Part 1], from $(12)_1$ we derive $\tilde{\bar{u}}_y(s,y,p)$ and $\tilde{\bar{v}}_y(s,y,p)$, and substituting these and $(12)_1$ into (9) and (10), we find A(s,p) and B(s,p) to be $(17)_1$, except that q(s,p) here contains the additional term $\sigma_0 s e^{-as}/\mu p$. Further, as in [6, Part 1], where we used the x = 0 edge conditions $(16)_1$ in f(s,y,p) and g(s,y,p) which reduced the latter to $(18)_1$, here the analog is the edge conditions (1) and (2) which gives

$$f(s,y,p) = k^2[s\bar{u}(0,y,p) - \sigma_{xI}^{HT}(0,y,p)/(\lambda + 2\mu)] + \bar{v}_y(0,y,p), \quad (22)$$

$$g(s,y,p) = k^{-2}[s\bar{v}(0,y,p) + (k^2 - 2)\,\bar{u}_y(0,y,p)] , \quad (23)$$

for $0 \leq y \leq d$. Now for the rest of the y-axis, $d \leq y \leq \infty$, we have the x = 0 edge conditions (11) and (13) which lead to

$$f(s,y,p) = k^2\bar{u}_x(0,y,p) + (k^2 - 1)\,\bar{v}_y(0,y,p) , \quad (24)$$

$$g(s,y,p) = k^{-2}\,\bar{v}(0,y,p) . \quad (25)$$

It follows that substituting the present A(s,p) and B(s,p) and (22)-(25) into $(12)_1$ defines the doubly transformed displacement solutions $\tilde{\bar{u}}(s,y,p)$ and $\tilde{\bar{v}}(s,y,p)$, and hence the quasi-formal solution $(6a)_1$ for the surface-breaking crack problem. This becomes the formal solution when the two time-transformed edge unknowns $\bar{u}(0,y,p)$ and $\bar{v}(0,y,p)$ become known, a process to be discussed later.

Indicated Contour Integration for Solution

As discussed in [6, Part 1], one needs a somewhat special contour in the s-plane to solve the present class of quarter-plane problems, one in which the so-called nonphysical roots and associated poles and residues of the generalized Rayleigh function are generated and, hence, can be exploited in the form of conditions on the solution ruling out unbounded and inadmissible events. A general contour that can do this is depicted in Fig. 3 of [6, Part 1]. The detail on the cuts and contours of this general contour will be left to the reader. Most important, however, are the contours involving the nonphysical zeros of the generalized Rayleigh function. Figures 4 and 5 of [6, Part 1], and related discussion, point out how the Fig. 3 of [6, Part 1] general contour is reduced through arguments of solution boundedness and wave speed restrictions ($c \leq c_d$) to path integrals.

Consistently, we now require that the contributions (residues) from the nonphysical poles, generated by the zeros of the generalized Rayleigh function, $s_{\pm j}(p) = \pm k_{Rj}$, $j = 2,3$ and $s_1(p) = k_{R1}$ must be

ruled out of the solution ($k_{Rj} = p/c_{Rj}$, where c_{Rj} is the wave speed). Of these, the residues at the poles $s_j(p) = k_{Rj}$, $j = 1,2,3$ are ruled out by the boundedness condition on the solution. The residues at $s_{-j}(p) = -k_{Rj}$, $j = 2,3$ are ruled out because the corresponding speeds of these Rayleigh wave events are greater than c_d. Hence, as the next section points out the residues for these five poles are set equal to zero. This eliminates the circular paths in Fig. 5 of [6, Part 1] for these contributions, generating four coupled integral equations that guarantee boundedness for the solution and the elimination of inadmissible events. Solution of these integral equations determines the edge unknowns in our problem, at least for wavefront (high frequency) events.

Conditions for Solution Boundedness and Inadmissible Events

In [6, Part 1] this section is concerned with the derivation of the four integral equations for the edge ($x = 0$) unknowns which begins with first establishing that $s_{\pm j}(p) = \pm k_{Rj}$, $j = 2,3$ and $s_1(p) = k_{R1}$ are zeros of the generalized Rayleigh function. An example, $s_2 = k_{R2}$ is considered, and shown to be a zero of this Rayleigh function, cf. $(19)_1$. The other nonphysical zeros, and the physical zero $s(p) = -k_{R1}$ follow suit.

The residues at $s = k_{R1}, \pm k_{Rj}$, $j = 2,3$ can be shown to be nonvanishing through the usual calculations.* These residues can then be set equal to zero by requiring that

$$A_N(s,p)\big|_{s = k_{R1}, \pm k_{Rj}} = B_N(s,p)\big|_{s = k_{R1}, \pm k_{Rj}} = 0, \quad j = 2,3, \qquad (22)_1$$

where $A_N(s,p)$, $B_N(s,p)$ are given in $(17)_1$. Now with $s_{\pm j}(p) = \pm k_{Rj}$, $j = 2,3$ and $s_1(p) = k_{R1}$ representing the five Rayleigh poles here, the two equations $(22)_1$ are expanded using $(17)_1$ and $(6d)_1$. After some algebra, and a simple integration on y for the coefficient of the input term $\sigma_0/\mu p$, the general integral equation is found to be

*These calculations are like those in the latter section dealing with the physical Rayleigh waves on the free edge $y = 0$, cf. [6, Part 2].

$$\int_0^\infty \left\{ \frac{s_j}{\alpha_j} \left[(k_s^2 - 2s_j^2) e^{-\alpha_j y} - 2\alpha_j \beta_j e^{-\beta_j y} \right] \left[k^2 s_j \bar{u}(0,y,p) + \bar{v}_y(0,y,p) \right] \right.$$

$$\left. + \left[(k_s^2 - 2s_j^2) e^{-\alpha_j y} + 2s_j^2 e^{-\beta_j y} \right] \left[s_j \bar{v}(0,y,p) + (k^2 - 2)\bar{u}_y(0,y,p) \right] \right\} dy$$

$$+ (k^2 - 2)k_s^2 \bar{u}(0,0,p) + \frac{k_s^2(k_s^2 - 2s_j^2)}{2s_j\alpha_j} \bar{v}(0,0,p) = \left(2 - \frac{k_s^2 - 2s_j^2}{\alpha_j^2} \right) \frac{s_j \sigma_0}{\mu p}, \quad (23)_1$$

where $s_j = s_j(p)$, $j = 1, \pm 2, \pm 3$. The s_j are basic to the definitions of the α_j and β_j.

Consider α_1 and β_1 first. From $(7)_1$ and $(8)_1$ we have, when $s_1 + k_{R1}$ (cf. Fig. 3 of 6, Part 1), $\alpha_1 = i(\rho_1\rho_2)^{1/2} = i(k_{R1}^2 - k_d^2)^{1/2}$ and $\beta_1 = i(\rho_3\rho_4)^{1/2} = i(k_{R1}^2 - k_s^2)^{1/2}$. Likewise, when $s_{\pm 2} = \pm k_{R2}$, $s_{\pm 3} = \pm k_{R3}$, along paths ℓ_3 and L_7, $(7)_1$ and $(8)_1$ show that $\alpha_{\pm 2} = (\rho_1\rho_2)^{1/2} = (k_d^2 - k_{R2}^2)^{1/2}$ and $\beta_{\pm 2} = -(\rho_3\rho_4)^{1/2} = -\bar{\beta}_{\pm 2} = -(k_s^2 - k_{R2}^2)^{1/2}$ with $\alpha_{\pm 3}$ and $\beta_{\pm 3}$ having the same forms as $\alpha_{\pm 2}$ and $\beta_{\pm 2}$ except that k_{R3} replaces k_{R2}. Equation $(23)_1$ represents five coupled integral equations for the two time-transformed edge displacement unknowns $\bar{u}(0,y,p)$, $\bar{v}(0,y,p)$ and their corner values $\bar{u}(0,0,p)$, $\bar{v}(0,0,p)$.

Now substituting the $j = 1$ terms, s_1, α_1, and β_1 above, into $(23)_1$, one finds it splits into two equations, the real and imaginary parts created by the imaginary nature of α_1 and β_1. These two real integral equations provide the definition of the time-transformed corner displacements $\bar{u}(0,0,p)$ and $\bar{v}(0,0,p)$ which is given by $(22)_1$. It follows that if these integral expressions for $\bar{u}(0,0,p)$ and $\bar{v}(0,0,p)$ are substituted into $(23)_1$, then there are just four integral equations involving only the time-transformed edge unknowns $\bar{u}(0,y,p)$, $\bar{v}(0,y,p)$, and related derivatives $\bar{u}_y(0,y,p)$ and $\bar{v}_y(0,y,p)$. These four remaining equations are parametric in $s_{\pm 2}$ and $s_{\pm 3}$, respectively, with related $\alpha_{\pm 2}$, $\beta_{\pm 2}$, $\alpha_{\pm 3}$ and $\beta_{\pm 3}$. This solution provides the information required to reduce the quasi-formal solution to the formal solution which can then be inverted by known exact and approximate solution techniques.

The analog of the above for the surface-breaking crack problem involves first the slight difference in A(s,p) and B(s,p) mentioned earlier, which affects A_N and B_N in $(22)_1$, $(17)_1$, and $(6d)_1$. The

stems from the spatially mixed boundary conditions along the y-axis for the present problem, i.e., $0 \leq y < d$ and $d \leq y < \infty$. The replacement, guided by the boundary conditions (11), (12), and (13), and the f(s,y,p) and g(s,y,p) terms, (22)-(25), along the y-axis, is

$$\int_0^d \left\{\frac{s_j}{\alpha_j}\left[(k_s^2 - 2s_j^2)e^{-\alpha_j y} - 2\alpha_j\beta_j e^{-\beta_j y}\right]\right.$$

$$\times \left[k^2\left\{s_j\bar{u}(0,y,p) - (\bar{\sigma}_{xI}^{HT}(0,y,p)/(\lambda+2\mu))\right\} + \bar{v}_y(0,y,p)\right]$$

$$\left. + \left[(k_s^2 - 2s_j^2)e^{-\alpha_j y} + 2s_j^2 e^{-\beta_j y}\right]\left[s_j\bar{v}(0,y,p) + (k^2-2)\,\bar{u}_y(0,y,p)\right]\right\}dy$$

$$\int_d^\infty \left\{\frac{s_j}{\alpha_j}\left[(k_2^2 - 2s_j^2)e^{-\alpha_j y} - 2\alpha_j\beta_j e^{-\beta_j y}\right]\left[k^2 u_x(0,y,p) + (k^2-1)\bar{v}_y(0,y,p)\right]\right.$$

$$\left. + \left[(k_s^2 - 2s_j^2)e^{-\alpha_j y} + 2s_j^2\, e^{-\beta_j y}\right]\left[s_j\bar{v}(0,y,p)\right]\right\}\,dy$$

$$+ (k^2-2)k_s^2\,\bar{u}(0,0,p) + \frac{k_s^2(k_s^2 - 2s_j^2)}{2s_j\alpha_j}\,\bar{v}(0,0,p) = (-\sigma_0 k_s^2\, e^{-as_j/\mu p}) \tag{26}$$

where $s_j = s_j(p)$, $j = 1,\pm2,\pm3$. The s_j are basic to the definitions of the α_j and β_j. The analog of $(24)_1$ for the present problem is

$$\begin{bmatrix}\bar{u}(0,0,p) - P(p)L(p)\\ \bar{v}(0,0,p) + Q(p)M(p)\end{bmatrix}$$

$$= -\begin{pmatrix}P(p)\\ Q(p)\end{pmatrix}\left\{\int_0^d\left\{\mp k_{R1}\left\{\left[(k_s^2 - 2k_{R1}^2)/|\alpha_1|\right]\begin{bmatrix}\sin|\alpha_1|y\\ \cos|\alpha_1|y\end{bmatrix}\right.\right.\right.$$

$$\left.\left.\left. + 2|\beta_1|\begin{bmatrix}\sin|\beta_1|y\\ \cos|\beta_1|y\end{bmatrix}\right\}\left\{k^2 k_{R1}\,\bar{u}(0,y,p) + \bar{v}_y(0,y,p)\right\}\right.\right.$$

$$\left.\left. + \left\{(k_s^2 - 2k_{R1}^2)\begin{bmatrix}\cos|\alpha_1|y\\ \sin|\alpha_1|y\end{bmatrix}\right.\right.$$

$$\left.\left.\left. + 2k_{R1}^2\begin{bmatrix}\cos|\beta_1|y\\ \sin|\beta_1|y\end{bmatrix}\right\}\left\{k_{R1}\bar{v}(0,y,p) + (k^2-2)\bar{u}_y(0,y,p)\right\}\right\}\,dy$$

$$+ \int_d^\infty \left\{ \mp k_{R1} \left\{ \left[(k_s^2 - 2k_{R1}^2)/|\alpha_1| \right] \begin{bmatrix} \sin|\alpha_1|y \\ \cos|\alpha_1|y \end{bmatrix} \right.\right.$$

$$\left. + 2|\beta_1| \begin{bmatrix} \sin|\beta_1|y \\ \cos|\beta_1|y \end{bmatrix} \right\} \left\{ k^2 \bar{u}_x(0,y,p) + (k^2 - 1)\bar{v}_y(0,y,p) \right\}$$

$$\left. + \left\{ (k_s^2 - 2k_{R1}^2) \begin{bmatrix} \cos|\alpha_1|y \\ \sin|\alpha_1|y \end{bmatrix} + 2k_{R1}^2 \begin{bmatrix} \cos|\beta_1|y \\ \sin|\beta_1|y \end{bmatrix} \right\} \left\{ k_{R1} \bar{v}(0,y,p) \right\} \right\} dy \Bigg\} \tag{27}$$

where

$$L(p) = -\frac{\sigma_0 p}{\mu c_s^2} e^{-ak_{R1}} ,$$

$$M(p) = \frac{\sigma_0}{\mu} \left[\frac{e^{-ap/c_d} k_{R1}}{(\pi a)^{3/2}(k^2 - 2)\sqrt{2c_d p}} \left(\frac{(k_s^2 - 2k_{R1}^2)|\beta_1| - 2|\alpha_1|^3}{|\alpha_1|^3 |\beta_1|} \right) \right] ,$$

$$P(p) = (k^2 - 2)^{-1} k_s^{-2} , \qquad Q(p) = 2k_{R1}|\alpha_1|/k_s^2(k_s^2 - 2k_{R1}^2) .$$

Now if $\bar{u}(0,0,p)$ and $\bar{v}(0,0,p)$ from (27) are substituted into (26), then there are just four integral equations, parametric in $s_{\pm 2}$, $s_{\pm 3}$, respectively, with related $\alpha_{\pm 2}$, $\beta_{\pm 2}$, $\alpha_{\pm 3}$, and $\beta_{\pm 3}$, involving only the time-transformed edge unknowns $\bar{u}(0,y,p)$, $\bar{v}(0,y,p)$ and related derivatives $\bar{u}_y(0,y,p)$, $\bar{v}_y(0,y,p)$ in the present problem. As in [6, Part 1], the solution of these four integral equations provides the time-transformed knowns needed to reduce the quasi-formal solution to the formal solution which can then be inverted by known exact and approximate solution techniques.

Determination of Time-Transformed Edge (x = 0) and Corner (x = y = 0) Unknowns for Wavefront Events and Their Inverses

As in [6, Part 1], to derive the time-transformed edge (x = 0) unknowns representing wavefront (high frequency events) we will use as a guide similar general features of related events from the elastic half-plane and waveguide problems. Indeed, we can construct forms for the time-transformed edge unknowns which will reduce the four integral equations to algebraic equations for the time-transformed p-dependent coefficients of these unknowns. In the present problems the time-transformed edge (x = 0) unknowns lead to diffracted waves propagating along the x = 0 edge (y-axis).

From the wavefront analysis work [8] on the plane strain semi-infinite plate, involving mixed pressure edge conditions, we assume at the dilatational wavefront, the time-transformed displacements $\bar{u}(0,y,p)$, $\bar{v}(0,y,p)$ are, respectively,

$$\bar{u}_d(0,y,p) \simeq A(p)y^{-1/2}e^{-k_d y}, \quad \bar{v}_d(0,y,p) \simeq B(p)y^{-1/2}e^{-k_d y} \tag{28}$$

from which we also have

$$\bar{u}_{yd}(0,y,p) \simeq -k_d A(p)y^{-1/2}e^{-k_d y}, \quad \bar{v}_{yd}(0,y,p) \simeq -k_d B(p)y^{-1/2}e^{-k_d y}, \tag{29}$$

both in $0 \leq y < d$, i.e., along the crack faces. It may be noted the $y^{-1/2}$ in these expressions is in agreement with the classical form for the propagation of two-dimensional surfaces of discontinuity in elastodynamics. The $\exp(-k_d y)$ through its shift operator nature guarantees the expected one-dimensional wave nature of these quantities, e.g., $u_d(0,y,p) \Longrightarrow u_d(0,y,t-y/c_d)$.

Consider next the Rayleigh wave disturbance on the edge $x = 0$. Here as in the half-plane problem one would expect a nondecaying in space (y) one-dimensional disturbance. Hence, it is assumed that

$$\bar{u}_R(0,y,p) = C(p)\exp(-k_{R1}y), \quad \bar{v}_R(0,y,p) = D(p)\exp(-k_{R1}y), \tag{30}$$

from which one also has

$$\begin{aligned} \bar{u}_{yR}(0,y,p) &= -k_{R1}\, C(p)\, \exp(-k_{R1}y), \\ \bar{v}_{yR}(0,y,p) &= -k_{R1}\, D(p)\, \exp(-k_{R1}y), \end{aligned} \tag{31}$$

both in $0 \leq y < d$, i.e., along the crack faces.

The edge of the crack at $y = d$ is a source of diffracted dilatational and Rayleigh surface wavefronts that propagate from $y = d$ to $y = 0$ (cf. Fig. 3), and indeed keep diffracting from $y = 0$ and $y = d$ ad infinitum as time progresses. Furthermore, the crack edge at $y = d$ generates the diffracted dilatational wavefronts that propagate in the domain $d \leq y < \infty$ from $y = d$ to ∞, ad infinitum, being generated by the diffracted dilatational wavefronts on the crack faces, when they reach the crack edge $y = d$ as time progresses. Since the boundary conditions in $d \leq y < \infty$ are mixed [$\sigma_{xy}(0,y,t) = u(0,y,t) = 0$], the Rayleigh surface waves are not present in $d \leq y < \infty$, cf. [7, Fig. 8.5].

For these additional diffracted wavefronts, assuming their time behavior is always the same as the basic wavefronts derived from the time transformed edge (x = 0) unknowns (28)-(31), we can derive these additional wavefronts from forms similar to (28)-(31). First, we have for the domain $d \leq y < \infty$,

$$\bar{u}_x(0,y,p) \simeq s\bar{u}_d(0,y,p) = sA(p)(y-d)^{-1/2} e^{-k_d(y-d)} , \tag{32}$$

$$\bar{v}_d(0,y,p) \simeq B(p)(y-d)^{-1/2} e^{-k_d(y-d)} , \tag{33}$$

and

$$\bar{v}_y(0,y,p) \simeq -k_d\bar{v}_d(0,y,p) . \tag{34}$$

The time-transformed edge (x = 0) unknowns for the first and higher order diffracting wavefronts in the domain of the crack are for the dilatational wavefronts,

$$\begin{aligned}
\bar{u}_{d1}(0,y,p) &\simeq A(p)y^{-1/2} e^{-k_d y} , && 0 \leq y \leq d, \\
\bar{u}_{d2}(0,y,p) &\simeq A(p)(d-y)^{-1/2} e^{-k_d(d-y)} , && 0 \leq d-y \leq d, \\
\bar{u}_{d3}(0,y,p) &\simeq A(p)(2d-y)^{-1/2} e^{-k_d(2d-y)} , && d \leq 2d-y \leq 2d,
\end{aligned} \tag{35}$$

where subscript $1,2,3\cdots n$ indicate the first, second, third, etc. transits of the associated wavefronts. Clearly, (35) is a series of terms for $\bar{u}_{dn}(0,y,p)$ with n being finite, since the inverse series will be finite for any fixed t. We note replacing A(p) in (35) with B(p) will result in a similar series of terms for $\bar{v}_{dn}(0,y,p)$.

It follows that the Rayleigh surface wavefronts have essentially the same form of time-transformed edge unknowns as in (35), but based on (30).

Concerning the time-transformed edge (x = 0) unknowns for the first and higher order diffracting dilatational wavefronts in the domain below the crack, we have

$$\begin{aligned}
\bar{u}_{x1}(0,y,p) &\simeq sA(p)(y-d)^{-1/2} e^{-k_d(y-d)} , && 0 \leq y-d < \infty , \\
\bar{u}_{x2}(0,y,p) &\simeq sA(p)(y-3d)^{-1/2} e^{-k_d(y-3d)} , && 0 \leq y-3d < \infty , \\
u_{x3}(0,y,p) &\simeq sA(p)(y-5d)^{-1/2} e^{-k_d(y-5d)} , && 0 \leq y-5d < \infty ,
\end{aligned} \tag{36}$$

where subscripts 1,3,5,$\cdots$n, indicate the first, second, third, etc. transits of the associated wavefronts. Again here we have a series of terms for $\bar{u}_{xn}(0,y,p)$ and $\bar{v}_{dn}(0,y,p)$ hence $\bar{v}_{yn}(0,y,p)$ from (34) [with B(p) for A(p) in (36)].

It follows then, neglecting the equivoluminal disturbance on the edge (x = 0) for the moment, that the r.h. sides of the expressions (28)-(36) may be substituted into the four integral equations obtained from (26) and (27), as discussed after (27). The simple integrations these terms provide reduce the four integral equations to four algebraic ones that determine the time-transformed coefficients A(p), B(p), C(p), and D(p) through Cramer's rule. The four algebraic equations are of the form

$$\hat{A}_j(s_j,p)A(p) + \hat{B}_j(s_j,p)B(p) + \hat{C}_j(s_j,p)C(p) + \hat{D}_j(s_j, p)D(p) = T_j(s_j,p) \quad , \tag{37}$$

where $\hat{A}_j$, $\hat{B}_j$, $\hat{C}_j$, and $\hat{D}_j$ are the coefficients of A(p), B(p), C(p), and D(p), respectively, and T_j represent the loading terms, with $j = \pm 2, \pm 3$. It is of interest now to derive the time-transformed coefficients corresponding to the first transit of the wavefronts in $0 \leq y \leq d$, and then inverting to get the time nature of these wavefronts. The first transit case is the simplest. We find for the dilatational displacement wavefronts on the edge x = 0,

$$\begin{matrix} u_d(0,y,t) \\ v_d(0,y,t) \end{matrix} \sim \pm(\sigma_0/\mu y^{1/2})\left[(2/\pi^{1/2})\left\{t - (y + c_d a/c_{R1})c_d^{-1}\right\}^{1/2} + (\tfrac{1}{2})\left\{t - (y+a)c_d^{-1}\right\}^2\right] \quad , \tag{38}$$

and the Rayleigh displacement wavefronts

$$\left\{\begin{matrix} u_R(0,y,t) \\ v_R(0,y,t) \end{matrix}\right\} \sim \pm(\sigma_0/\mu)\left\{H\left[t - (y+a)c_{R1}^{-1}\right] + (4/3\pi^{1/2})\left[t - (y + c_{R1}a/c_d)c_{R1}^{-1}\right]^{3/2}\right\} \quad , \tag{39}$$

except for certain constants akin to A, B, C, and D in (A.1) of the Appendix of (6, Part 1). The derivation of the time-transformed coefficients corresponding to the second and higher order transits of the wavefronts over the crack, $0 \leq y \leq d$, and over the domain below the crack, $d \leq y \leq \infty$, is algebraically more complicated due

to the multiple exponential decay terms occurring in the coefficients of A(p), B(p), C(p), and D(p), associated with each higher order wavefront transit, e.g.,

$$I_d^{cr} = [\pi/(\alpha_j + k_d)]^{1/2} + [\pi/(k_d - \alpha_j)]^{1/2} \sum_{n=1,2,3\cdots}^{\infty} e^{-nd\alpha_j}, \quad (40)$$

$$I_d^{bc} = [\pi/(\alpha_j + k_d)]^{1/2} \sum_{n=1,3,5\cdots}^{\infty} e^{-nd\alpha_j}, \quad (41)$$

where subscripts on the I's indicate dilatational wavefronts, and super cr and super bc indicate "along the crack" and "below the crack", respectively. Note that the first term in (40), associated with the first wavefront transit does not have exponential decay. It and other similar terms will be associated with first order terms in the solution which have $y^{-1/2}$ decay, e.g., (38).

Concerning the two-sided equivoluminal wavefronts on the edge, $x = 0$, one would expect the present method to yield them as in [6, Part 2] in terms of constants like A, B, C, and D in (A.1) of [6, Part 1]. In effect this says the dilatational and Rayleigh wavefronts (on $x = 0$) generate these equivoluminal wavefronts on the crack faces and below, as well as the other wavefronts in the problem. Also, as pointed out in [6, Part 1], interesting is the fact that the two-sided equivoluminal wavefronts on the crack faces have the same time behavior as the dilatational wavefronts there, which is also true in Lamb's plane strain problem, cf. [7, Eqs. (6.52), (6.53)]. One might expect then, in the present problem, to find the same behavior over the first transit of the crack.

Further, we have the input of the two-sided equivoluminal wavefronts on the crack faces, stemming from the source function at the point $x = a$, $y = 0$ shown in Fig. 3. In this case, r in this figure touches a point y on the crack face associated with the incident two-sided equivoluminal wavefronts SV_I (E shown in Fig. 3 at an earlier position on the surface to the left of the source) and the reflected SV_R and P_R wavefronts. Recalling from (11) that the shear stress vanishes everywhere on the edge $x = 0$, we have

$$\bar{\sigma}_{xy}(0,y,p)/\mu = \bar{u}_y(0,y,p) + \bar{v}_x(0,y,p) = 0, \quad 0 \le y < \infty, \quad (42)$$

and so over the crack faces $0 \le y < d$. Hence, we can prove (42) and in the process set down the nature of the incident and total incident system of the two-sided equivoluminal wavefronts represented by $u^H_{ysI}(x,y,t)$, $u^{HT}_{ysI}(x,y,t)$, $v^H_{xSI}(x,y,t)$, and $v^{HT}_{xSI}(x,y,t)$. From eq. (6.15) in [7] we write,

$$\begin{bmatrix} \bar{u}^{H}_{yI}(x,y,p) \\ \bar{v}^{H}_{xI}(x,y,p) \end{bmatrix} = \frac{\sigma_o \bar{H}(p)}{2\pi\mu} \int_{-\infty}^{\infty} \begin{bmatrix} \partial/\partial y \\ \partial/\partial x \end{bmatrix} \left[\begin{Bmatrix} f_s(\zeta) \\ h_s(\zeta) \end{Bmatrix} e^{-pg_s(\zeta)} \right] d\zeta \qquad (43)$$

where

$$g_s(\zeta) = (1/c_d)[\eta_s'(\zeta)y - i\zeta(a-x)]$$

$$f_s(\zeta) = i2\zeta\, \eta_d'(\zeta)\, \eta_s'(\zeta)/R(\zeta)$$

$$h_s(\zeta) = 2\zeta^2 \eta_d'(\zeta)/R(\zeta)$$

and

$$R(\zeta) = (k^2 + 2\zeta^2)^2 - 4\zeta^2\, \eta_d'(\zeta)\, \eta_d'(\zeta) \ .$$

Carrying out the differentiations in (43) reduces it to the two components involving $f_s(\zeta)$ and $h_s(\zeta)$. It follows that

$$\begin{bmatrix} \bar{u}^{H}_{ysI}(x,y,p) \\ \bar{v}_{xsI}(x,y,p) \end{bmatrix} = -\frac{\sigma_o}{2\pi\mu c_d} \int_{-\infty}^{\infty} \begin{bmatrix} \eta_s'(\zeta)\, f_s(\zeta) \\ i\zeta h_s(\zeta) \end{bmatrix} e^{-pg_s(\zeta)}\, d\zeta$$

which becomes

$$\begin{bmatrix} \bar{u}^{H}_{ysI}(x,y,p) \\ \bar{v}^{H}_{xsI}(x,y,p) \end{bmatrix} = -\frac{\sigma_o}{\pi\mu c_d} \int_{r/c_s}^{\infty} \mathrm{Re} \left\{ \begin{bmatrix} \eta_s'(\zeta)\, f_s(\zeta) \\ i\zeta h_s(\zeta) \end{bmatrix} \frac{d\zeta_s}{dt} \right\} e^{-pt}\, dt, \qquad (44)$$

hence from (6.59) in [7] and (44), we have

$$\begin{bmatrix} u^{H}_{ysI}(x,y,t) \\ v^{H}_{xsI}(x,y,t) \end{bmatrix} = -\frac{\sigma_o}{\pi\mu c_d} \mathrm{Re} \left\{ \begin{bmatrix} \eta_s'(\zeta)\, f_s(\zeta) \\ i\zeta h_s(\zeta) \end{bmatrix} \Big/ g_s'[\zeta(t)] \right\} H(t - \frac{r}{c_s}) \qquad (45)$$

for $r/c_s \leq t < \infty$. Now, since $\zeta = -i\zeta_o = -ik\sin\theta$ is the saddle point, (45) becomes

$$\begin{bmatrix} u^{H}_{ysI}(x,y,t) \\ v^{H}_{xsI}(x,y,t) \end{bmatrix} = \frac{\sigma_o}{\pi\mu c_d} \mathrm{Re} \left\{ \begin{bmatrix} \eta_s'(-i\zeta_o)\, f_s(-i\zeta_o) \\ -\zeta_o h_s(-i\zeta_o) \end{bmatrix} \Big/ g_s'[\zeta(t)] \right\} H(t - \frac{r}{c_s}) \qquad (46)$$

where one can reduce these solutions further using $\eta_d'[-i\zeta_o] = (1-\zeta_o^2)^{1/2} = -i(k^2\sin^2\theta - 1)^{1/2}$, and $\eta_s'[-i\zeta_o] = k(1-\sin^2\theta)^{1/2} = k\cos\theta$, noting that η_d' has to be negative imaginary since that is its basic value in the fourth quadrant of the ζ-plane. Now we expand away from the saddle point and the minimum time, $t = r/c_s + \varepsilon$, $\varepsilon \ll 1$ and along -a' shown in Fig. 1 of [6, Part 2], i.e.,

$$t = g_s(-i\zeta_o) + \frac{g''(-i\zeta_o)}{2}(\zeta + i\zeta_o)^2 + \cdots$$

$$\simeq r/c_s + \frac{g''(-i\zeta_o)}{2}(\zeta + i\zeta_o)^2 + \cdots \qquad (47)$$

or

$$\zeta + i\zeta_o = [2(t - r/c_s)/g_s''(-i\zeta_o)]^{1/2} \quad . \qquad (48)$$

From (47) and (48),

$$g_s'(\zeta) \simeq g''(-i\zeta_o)(\zeta + i\zeta_o) = [2g_s''(-i\zeta_o)(t - r/c_s)]^{1/2} \quad . \qquad (49)$$

This generates the first case, the regular wavefront part. Now for the second case, we expand along -b' (L_3) in Fig. 1 of [6, Part 1] and find the precursor part of our two-sided wavefront, through

$$\zeta + i\zeta_o \simeq i[2(r/c_s - t)\,/\,g_s''(-i\zeta_o)]^{1/2} \quad , \qquad (50)$$

and therefore

$$g_s'(\zeta) \simeq i[2g_s''(-i\zeta_o)(r/c_s - t)]^{1/2} \quad . \qquad (51)$$

The function $g_s''(-i\zeta_o) = 2c_s r/c_d^2\cos^2\theta$ is easily derived. Hence, from (46) we can set down the incident two-sided equivoluminal wavefronts for u^H_{ysI} and v^H_{xsI} along the crack faces. For the regular wavefront (first case) we have from (47)-(49),

$$\begin{bmatrix} u^H_{ysI}(0,y,t) \\ v^H_{xsI}(0,y,t) \end{bmatrix} = \frac{\sigma_o}{\pi\mu c_d}\,\mathrm{Re}\left\{ \begin{bmatrix} \eta_s'(-i\zeta_o)\ f_s(-i\zeta_o) \\ -\zeta_o h_s(-i\zeta_o) \end{bmatrix} \right\}$$

$$\Big/ [(2c_s r/c_d^2\cos^2\theta)(t - r/c_s)]^{1/2}\, H(t - \tfrac{r}{c_s}) \quad . \qquad (52a)$$

For the precursor wavefront (the second case), we have from (50) and (51),

$$\begin{bmatrix} u^H_{ysI}(0,y,t) \\ v^H_{xsI}(0,y,t) \end{bmatrix} = \frac{\sigma_o}{\pi\mu c_d} \operatorname{Re}\left\{ \begin{bmatrix} \eta_s'(-i\zeta_o) f_s(-i\zeta_o) \\ -\zeta_o\, h_s(i\zeta_o) \end{bmatrix} \right\}$$

$$\Big/ [(2c_s r/c_d^2 \cos^2\theta)(r/c_s - t)]^{1/2}\, H(r - c_s t) \cdot \tag{52b}$$

At this point we must derive $u^{HT}_{ysI}(0,y,t)$ and $v^{HT}_{xsI}(0,y,t)$ which involves the reflection coefficients for SV wave incidence, SV_I representing $u^H_{ysI}(0,y,t)$ and $v^H_{xsI}(0,y,t)$. Reference [7], eq. (3.25) gives these relations for the ordinary reflection of SV waves from a free surface of an elastic half plane in plane strain. They are

$$\frac{SV_R}{SV_I} = \frac{\sin 2\alpha \sin 2\beta - k^2 \cos^2 2\beta}{\sin 2\alpha \sin 2\beta + k^2 \cos^2 2\beta}$$

$$\frac{P_R}{SV_I} = \frac{k^2 \sin 4\beta}{\sin 2\alpha \sin 2\beta + k^2 \cos^2 2\beta} \tag{53}$$

where $\beta = \pi/2 - \theta$ is the angle of incidence w.r.t. the y-axis of SV_I and angle of reflection of SV_R, and α is the angle of reflection of P_R, cf. Fig. 3. Since $k > 1$, we have a real value of α as long as $0 \le \sin\beta \le 1/k$ or equivalently $0 \le \beta \le \sin^{-1}(1/k) = \beta_{cr}$, the critical angle, cf. [7, §3.1.2.2.] Now with $\sin\beta = \sin(\pi/2 - \theta) = \cos\theta$, $\cos\beta = \sin\theta$, $\sin\alpha = k\cos\theta$, and using these relations we have from (53),

$$\frac{SV_R}{SV_I} = \frac{4k \sin\theta \cos^2\theta (1 - k^2\cos^2\theta)^{1/2} - k^2(1 - 2\cos^2\theta)^2}{4k \sin\theta \cos^2\theta (1 - k^2\cos^2\theta)^{1/2} + k^2(1 - 2\cos^2\theta)^2}$$

$$\frac{P_R}{SV_I} = \frac{4k^2 \cos\theta \sin\theta (1 - 2\cos^2\theta)}{4k \sin\theta \cos^2\theta (1 - k^2\cos^2\theta)^{1/2} + k^2(1 - 2\cos^2\theta)^2} \tag{54}$$

Hence, we have from SV_I and (54),

$$SV_I^T = SV_I + SV_R + P_R = (1 + SV_R/SV_I + P_R/SV_I)\ SV_I$$

$$= 4\left\{\frac{[2\cos\theta(1-k^2\cos^2\theta)^{1/2} + k(1-2\cos^2\theta)]\sin\theta\cos\theta}{4\sin\theta\cos^2\theta(1-k^2\cos^2\theta)^{1/2} + k(1-2\cos^2\theta)}\right\} SV_I \qquad (55)$$

For the case of reflection of SV waves at critical angles of incidence, there is no ordinary reflected P wave in the range $\beta_{cr} < \beta < \pi/2$. For these larger β angles we have in the present problem a case of <u>total reflection</u> which is discussed at length in [7, §3.1.4.5]. It is the counterpart of (55).

Now SV_I^T in (55) can be identified with each of the incident displacement gradient wavefronts in (52a,b). Hence it follows that $u^{HT}_{ysI}(0,y,t)$ and $v^{HT}_{xsI}(0,y,t)$ are just the products of $u^{H}_{ysI}(0,y,t)$ and $v^{H}_{xsI}(0,y,t)$ in (52a,b) and the coefficient of SV_I in (55). These total incident systems of wavefronts enable us to prove directly the boundary condition (1), $\sigma_{xy}(0,y,t)=0$, over the crack faces, i.e., we prove (42) through

$$\sigma^{HT}_{xysI}(0,y,t)/\mu = u^{HT}_{ysI}(0,y,t) + v^{HT}_{xsI}(0,y,t) = 0,\ 0 \le y < d\ . \qquad (56)$$

From (52a) we have

$$\sigma^{H}_{xysI}(0,y,t)/\mu = u^{H}_{ysI}(0,y,t) + v^{H}_{xsI}(0,y,t)$$

$$= \frac{\sigma_o}{\pi\mu c_d}\left\{\frac{\mathrm{Re}[\eta_s'(-i\zeta_o)f_s(-i\zeta_o) - \zeta_o h_s(-i\zeta_o)]}{[(2c_s r/c_d^2\cos^2\theta)\ (t - r/c_s)]^{1/2}}\right\} H(t - r/c_s)$$

$$= \frac{\sigma_o}{2\pi\mu c_d}\left[\left\{\begin{matrix}\text{in}\\ \text{the}\\ \text{above}\end{matrix}\right\} + \left\{\begin{matrix}\text{in}\\ \text{the}\\ \text{above}\end{matrix}\right\}\right] H(t - r/c_s) = 0\ . \qquad (57)$$

Now identifying the last line of (57) with the first line shows that $u^{H}_{ysI}(0,y,t) = -v^{H}_{xsI}(0,y,t)$, hence proving (57). It follows that if we multiply the expressions in (57) by the coefficient of SV_I in (55) we will obtain (56) which was to be proved, i.e., $u^{HT}_{ysI}(0,y,t) = -v^{HT}_{xsI}(0,y,t)$.

It is easily seen by inspection of (52b) that proof for it models that just set down for (52a) and hence completes our proof of (42).

To determine the corner displacements u(0,0,t) and v(0,0,t), the r.h. sides of (28)-(36) are substituted into (27), resulting in real integrals of the types

$$\int_0^\infty \begin{Bmatrix} \sin my \\ \cos my \end{Bmatrix} \frac{e^{-ay}}{\sqrt{y}}\, dy = \left[\frac{\pi}{2(a^2+m^2)}\right]^{1/2} \begin{bmatrix} [(a^2+m^2)^{1/2}-a]^{1/2} \\ [(a^2+m^2)^{1/2}+a]^{1/2} \end{bmatrix},$$

$$\int_0^\infty \begin{Bmatrix} \sin my \\ \cos my \end{Bmatrix} e^{-ay}\, dy = \begin{Bmatrix} m \\ a \end{Bmatrix} \Big/ (a^2+m^2) \quad , \tag{58}$$

where a and m are > 0. The r.h. sides of (58) therefore reduce (27) to algebraic equations for $\bar{u}(0,0,p)$ and $\bar{v}(0,0,p)$ involving A(p), B(p), C(p), and D(p) which, using the r.h. sides of these four time-transformed coefficients will yield $\bar{u}(0,0,p)$ and $\bar{v}(0,0,p)$ where constants like $\hat{u},\hat{v}$ in (A.2) of the Appendix of [6, Part 1] would be involved. It follows that the corner displacements are of the form

$$u(0,0,t) = U(t) \ , \quad v(0,0,t) = V(t) \tag{59}$$

with corresponding velocities and accelerations.

The Formal Solution for the Time-Transformed Displacements $\bar{u}(x,y,p)$ and $\bar{v}(x,y,p)$

With the time-transformed edge (x = 0 unknowns in (28)-(36) now determined by the solution of the four algebraic equations (37) for A(p), B(p), C(p), and D(p), and similarly the time-transformed corner displacements $\bar{u}(0,0,p)$ and $\bar{v}(0,0,p)$, the quasi-formal solutions for the displacements u(x,y,t) and v(x,y,t), like $(6a,b,c,d)_1$ become the formal solutions for wavefront (high frequency) events for these displacements. It follows that these formal solutions in the present problem can be written in the form of those in $(35a)_1$ and $(35b)_1$. Further, with the aid of the principle of reflection in complex variables, the present analog of $(35a)_1$ and $(35b)_1$ can be reduced to real equations for $\bar{u}(x,y,p)$ and $\bar{v}(x,y,p)$ through complex conjugation. The result in [6, Part 1] is given by $(43)_1$, i.e.,

$$\begin{Bmatrix} \bar{u}(x,y,p) \\ \bar{v}(x,y,p) \end{Bmatrix} = \frac{1}{\pi} \int_{Br_{sL}} \mathrm{Im} \left\{ \begin{bmatrix} A_u(s,p) \\ A_v(s,p) \end{bmatrix} ds \right\} \tag{60}$$

where A_u and A_v are the integrands of the first integral on the r.h.s. of $(35a)_1$ for $\bar{u}(x,y,p)$ and $\bar{v}(x,y,p)$, respectively. The present problem would have a similar result.

Inversion of the Time-Transformed Displacements $\bar{u}(x,y,p)$, $\bar{v}(x,y,p)$ by the Cagniard-de Hoop Technique

The formal solutions for $\bar{u}(x,y,p)$ and $\bar{v}(x,y,p)$ of the surface-breaking crack problem can be inverted by the now well-known Cagniard-de Hoop technique which was used for the problem in [6, Part 1] and discussed there. Most important for the reader is the material associated with $(44)_1$-$(47)_1$ and Fig. 6 there, setting down the integrals in $(45)_1$ for $\bar{u}(x,y,p)$ and $\bar{v}(x,y,p)$ along with discussions of inversions of these integrals through transformations generating new paths of integration and associated singularities.

Wavefront Events in the Surface-Breaking Crack Problem

In [6, Part 2] the wavefront events in the edge uniform pressure problem, cf. Fig. 1 of [6, Part 1], were derived through further steps in the Cagniard-de Hoop inversion of $(45)_1$ and the related asymptotic method in [8]. In the interior of the quarter plane the events included for the displacements, velocities and accelerations, the dilatational wavefronts, the two-sided equivoluminal and head wavefronts in the two critical shear regions associated with the edges $x = 0$ and $y = 0$, and of course the plane dilatational wavefront from the edge $x = 0$ input. The events on the edges of the quarter plane included, for $y = 0$, the wavefronts just discussed for the interior and, in addition, the Rayleigh wavefronts. Concerning the loaded edge $x = 0$, $(29)_1$ and $(30)_1$ have already defined the dilatational and Rayleigh wavefronts. However, as pointed out in [6, Part 1], the present asymptotic method also yields the two-sided equivoluminal and head wavefronts on the loaded edge, $x = 0$. Further, we have the input of the two-sided equivoluminal wavefronts on the crack faces, stemming from the source function at the point $x = a$, $y = 0$ shown in Fig. 3. This work may be found in the material associated with (43)-(58). Finally, we will be seeking similar wavefront events for the present problem and the subsurface crack, which will be the subject of forthcoming papers.

REFERENCES

1. J.D. Achenbach,L.M. Keer and D.A. Mendelsohn, Elastodynamic analysis of an edge crack, J. Appl. Mech., Trans. ASME, 47:551, 1980.
2. D.A. Mendelsohn, J.D. Achenbach and L.M. Keer, Scattering of elastic waves by a surface-breaking crack, Wave Motion, 2:277, 1980.
3. T. Kundu and A.K. Mal, Diffraction of elastic waves by a surface crack on a plate, J. Appl. Mech., Trans. ASME, 48: 570, 1981.
4. J.D. Achenbach and R.J. Brind, Scattering of surface waves by a subsurface crack, J. Sound and Vibration, 76:43, 1981.
5. Y.H. Pao, editor, Elastic waves and non-destructive testing of materials, ASME Monograph, AMD-Vol. 29.
6. J. Miklowitz, Wavefront analysis in the nonseparable elastodynamic quarter-plane problems, I. Part 1: The general method; Part 2: Wavefront events in the edge uniform pressure problem; in press, J. Appl. Mech., Trans. ASME, Papers 82-WA/APM-12 and 82-WA/APM-13.
7. J. Miklowitz, The theory of Elastic Waves and Wavguides, North-Holland Publishing Co., Amsterdam, New York and Oxford, 1978.
8. R.L. Rosenfeld and J. Miklowitz, Wavefrnts in elastic rods and plates, Proc. 4th U.S. National Congress of Appl. Mech. 1, ASME, New York, 293-303, 1962.